Photoabsorption for helium, lithium, and beryllium atoms in the random-phase approximation with exchange

M. Ya. Amusia and N. A. Cherepkov
A. F. Ioffe Physical-Technical Institute of the Academy of Sciences of the USSR, Leningrad, USSR

Dj. Živanović and V. Radojević
Laboratory for Theoretical Physics, Boris Kidrich Institute, Belgrade, Yugoslavia
(Received 29 July 1975; revised manuscript received 16 December 1975)

The photoionization cross sections and the oscillator strengths for helium, lithium, and beryllium atoms are calculated in the framework of the random-phase approximation with exchange. The energy-level shift for discrete transitions is taken into account consistently in this approximation. The results are compared with other many-body calculations and with the experimental data. The comparison shows that the random-phase approximation with exchange can even be used for systems with a small number of particles.

I. INTRODUCTION

Many-body effects in the photoionization and photoexcitation of heavier atoms, particularly in the noble gases, have been investigated with success in the framework of the random-phase approximation with exchange (RPAE).[1-3] The response of these many-electron systems to a fast electron (instead of a photon) acting as a probe has been treated successfully in the RPAE as well.[4] This approximation takes into account the contribution of those Feynman diagrams that are dominant in the case of a dense finite system; with some justification, the electron shells in heavier atoms can be considered as a dense electron gas. The lightest atoms (He, Li, Be) certainly are not a dense electron gas; indeed, for these atoms the many-body perturbation theory is generally successful.[5-8] It is therefore interesting to investigate the correlation effects in the lightest atoms using the RPAE in order to see whether this approximation can be used even for systems with a small number of particles.

The use of the RPAE also has some practical advantages. In fact, using the multiple-basis-set technique[9] the contribution of an infinite series of diagrams can be represented by a single "renormalized" diagram; by taking such diagrams into account up to a certain order, one does much better than with just a perturbation calculation. But even so, several diagrams have to be calculated, while in the RPAE the contribution of all diagrams of the selected infinite class (among them, all first order) is obtained at once by solving the RPAE integral equation. Unfortunately, uncompensated exclusion-principle-violating (EPV) diagrams are then taken into account as well; this is the price to be paid for not having to calculate diagrams one by one.

In this paper an investigation of the photoeffect on the lightest atoms in the RPAE is presented. A preliminary report on these investigations was presented elsewhere.[10] In Sec. II we outline the theoretical framework for treating the response of the many-body system (atom) to an external perturbation (photon). In Sec. III the methods of numerical calculation are described, particularly those concerning the manner of solving the RPAE equation. Finally, in Sec. IV we present the results of our calculation of the photoionization cross section and the discrete transition oscillator strengths, and compare them with other many-body calculations and with experimental data. Throughout the present paper atomic units ($\hbar = m = e = 1$) are used except in figures, where energy is expressed in rydbergs.

II. THEORY

The interaction between the electrons of an atom and the external electromagnetic field is described by the Hamiltonian

$$H' = \sum_{\vec{k}\lambda} \vec{A}_{\vec{k}\lambda} \cdot \vec{J}_{-\vec{k}}, \tag{1}$$

where $\vec{A}_{\vec{k}}$ (in the Coulomb gauge, $\vec{k} \cdot \vec{A}_{\vec{k}} = 0$) describes photons of momentum $\vec{k}$ and polarization λ, and $\vec{J}_{\vec{k}}$ denotes the Fourier transform of the electron current density,

$$\vec{J}(\vec{r}) = \frac{1}{2} \sum_{i=1}^{N} [\vec{p}_i \delta(\vec{r} - \vec{r}_i) + \delta(\vec{r} - \vec{r}_i)\vec{p}_i], \tag{2}$$

where $\vec{p}_i$ and $\vec{r}_i$ are the momentum and the posi-

tion of the ith electron. We consider only the one-photon processes; thus the transition probabilities are calculated in first order in H'. The photoionization cross section (to an arbitrary final state $|\Psi_n\rangle$) is

$$\sigma(\omega)=\frac{4\pi^2}{\omega c}\sum_n |\langle\Psi_n|J^{\perp}_{-\vec{k}}|\Psi_0\rangle|^2\delta(E_n-E_0-\omega), \quad (3)$$

where ω is the energy of the photon and $J^{\perp}_{\vec{k}}$ denotes the transversal component of $\vec{J}_{\vec{k}}$.

The cross section (3) is related to the current density correlation function[11] $S(k,t)$ defined by

$$iS(k,t)=\langle\Psi_0|T\{J^{\perp}_{\vec{k}}(t)J^{\perp}_{-\vec{k}}(0)\}|\Psi_0\rangle; \quad (4)$$

the operator $J^{\perp}_{\vec{k}}(t)$ is given in the Heisenberg representation determined by the atomic Hamiltonian H_{at}, and T is the time-ordering operator. Because of the rotation invariance of H_{at}, $S(k,t)$ is independent of the orientation of $\vec{k}$. Comparing the Lehmann representation of $S(k,t)$ and (3), one sees immediately that

$$\sigma(\omega)=-(4\pi/\omega c)\,\text{Im}S(k,\omega), \quad (5)$$

where $S(k,\omega)$ is the Fourier transform of $S(k,t)$.

If the condition for the validity of the dipole approximation ($kR\ll 1$, R being the atomic radius) is fulfilled, the electron current density $\vec{J}_{\vec{k}}$ can be simplified considerably:

$$\vec{J}_{\vec{k}}\approx\vec{J}_{\vec{k}=0}\equiv\vec{P}=i[H_{\text{at}},\vec{D}]; \quad (6)$$

$\vec{P}=\sum_{i=1}^N\vec{p}_i$ is the total momentum of electrons and $\vec{D}=\sum_{i=1}^N\vec{r}_i$ is the dipole momentum of the atom. Using the relation between matrix elements of those operators taken with respect to eigenstates of H_{at}, one may choose either the velocity form (∇ form) or the length form (r form) of the current matrix elements in the dipole approximation. Those two forms are equivalent not only for the exact (local) Hamiltonian H_{at} but for the RPAE as well. The ∇ form makes $S(k=0,\omega)\equiv S(\omega)$ a total momentum correlation function, while the r form makes it a dipole momentum correlation function, closely related to the dipole polarizability $\alpha(\omega)$, so that $\sigma(\omega)$ can be expressed also in terms of $\text{Im}\alpha(\omega)$.[12,13]

The correlation function $S(\omega)$ can be related to $\Pi_{\lambda\mu,\alpha\beta}(\omega)$, the Fourier transform of the polarization propagator $\Pi_{\lambda\mu,\alpha\beta}(t,t')$;[14] λ, μ, α, and β denote the single-particle states $|\alpha\rangle=|nlms\rangle$, etc. This is essentially the two-particle Green's function of the many-electron system. The expression for $S(\omega)$ is

$$S(\omega)=\sum_{\lambda\mu\alpha\beta}\langle\mu|d^\dagger|\lambda\rangle\,\Pi_{\lambda\mu,\alpha\beta}(\omega)\,\langle\alpha|d|\beta\rangle, \quad (7)$$

where (in the dipole approximation)

$$d=\begin{cases} d_\nabla\equiv ip^\perp \\ d_r\equiv\omega r^\perp . \end{cases} \quad (8)$$

Also, (7) can be written in matrix form,

$$S(\omega)=d^\dagger\Pi(\omega)d, \quad (9)$$

where the one-column matrix d ($d_s\equiv d_{\alpha\beta}\equiv\langle\alpha|d|\beta\rangle$) and the square matrix $\Pi(\omega)$ are labeled by an ordered pair of the particle-hole states: $s=(\alpha,\beta)$; $\alpha>F$, $\beta\le F$, or $\alpha\le F$, $\beta>F$ [$\alpha\le F$ and $\alpha>F$ denote occupied (hole) and unoccupied (particle) states, respectively]. The correlation function can be represented by Feynman diagrams, as shown in Fig. 1.

For the photoexcitation, the transition probability to a discrete state of the atom can be expressed in terms of the oscillator strength

$$f_n=2\omega_n|\langle\Psi_n|D^\perp|\Psi_0\rangle|^2. \quad (10)$$

This quantity, originally defined in the r form, can be expressed in the ∇ form as well. From the Lehmann representation of the correlation function one obtains directly

$$f_n=(2/\omega_n)\,\text{Res}S(\omega_n), \quad (11)$$

where $\text{Res}S(\omega_n)$ denotes the residue of $S(\omega)$ at its pole $\omega_n=E_n-E_0$.

An approximate value for $S(\omega)$ is obtained by selecting and summing a subclass of Feynman diagrams; an approximate value for $\sigma(\omega)$ or f_n is then obtained from $S(\omega)$.

Taking the free polarization propagator

$$\Pi^0_{\lambda\mu,\alpha\beta}(\omega)=\frac{n_\beta-n_\alpha}{\omega-\epsilon_\alpha+\epsilon_\beta+i(n_\beta-n_\alpha)\eta}\,\delta_{\lambda\alpha}\delta_{\mu\beta}, \quad (12)$$

where ϵ_α and ϵ_β are the single-particle energies

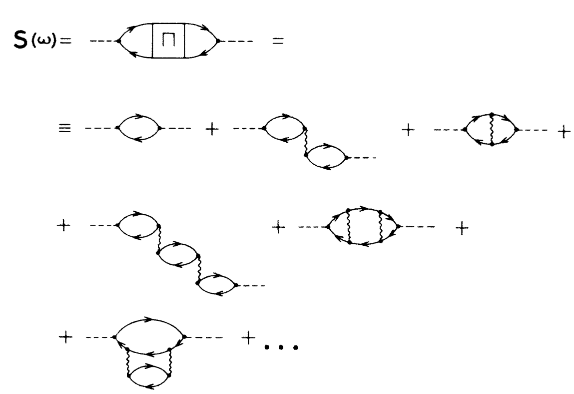

FIG. 1. Feynman diagrams for the correlation function $S(\omega)$, Eq. (7).

and n_α and n_β are the corresponding occupation numbers ($n_\alpha = 1$ for $\alpha \leq F$ and $n_\alpha = 0$ for $\alpha > F$), the single-particle approximation for $\sigma(\omega)$ or f_n is obtained. In our calculations the correlations are taken into account in the framework of the RPAE. The RPAE form of $\Pi(\omega)$ is

$$\Pi(\omega) = \Pi^0(\omega) + \Pi^0(\omega)\Gamma(\omega)\Pi^0(\omega), \tag{13}$$

where the effective interaction $\Gamma(\omega)$ satisfies the equation

$$\Gamma(\omega) = U + U\Pi^0\Gamma(\omega), \tag{14}$$

U being the antisymmetrized Coulomb interaction matrix element

$$U_{\lambda\mu,\alpha\beta} = \langle\lambda\beta|r_{12}^{-1}|\mu\alpha\rangle - \langle\lambda\beta|r_{12}^{-1}|\alpha\mu\rangle. \tag{15}$$

The matrix equations hereafter are to be understood in the same sense as (9).

We express $S(\omega)$ in terms of the renormalized photon vertex $\mathfrak{D}(\omega)$ defined by

$$\mathfrak{D}(\omega) = d + \Gamma(\omega)\Pi^0(\omega)d \tag{16}$$

and satisfying the equation

$$\mathfrak{D}(\omega) = d + U\Pi^0(\omega)\mathfrak{D}(\omega). \tag{17}$$

Equations (16) and (17) are represented diagramatically in Fig. 2. From (9), (13), and (16) one gets

$$S(\omega) = d^\dagger\Pi^0(\omega)\mathfrak{D}(\omega). \tag{18}$$

Then $\sigma(\omega)$ and f_n can be expressed in terms of $\mathfrak{D}(\omega)$, obtained by solving (17). From (17) and (18) one obtains

$$S(\omega) = \mathfrak{D}(\omega)^\dagger\Pi^0(\omega)\mathfrak{D}(\omega) - \mathfrak{D}(\omega)^\dagger\Pi^0(\omega)^\dagger U\Pi^0(\omega)\mathfrak{D}(\omega). \tag{19}$$

The second term on the right-hand side is real, owing to the Hermiticity of U. Therefore (for $\omega > 0$)

$$\mathrm{Im}S(\omega) = \mathrm{Im}\mathfrak{D}(\omega)^\dagger\Pi^0(\omega)\mathfrak{D}(\omega) = -\pi\sum_{\substack{\alpha>F\\ \beta\leq F}} |\mathfrak{D}_{\alpha\beta}(\omega)|^2\delta(\omega - \epsilon_\alpha + \epsilon_\beta) \tag{20}$$

and

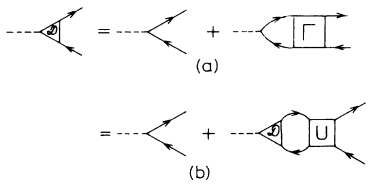

FIG. 2. Diagramatic representation of (a) Eq. (16), defining the renormalized photon vertex $\mathfrak{D}(\omega)$; and (b) Eq. (17), satisfied by $\mathfrak{D}(\omega)$.

$$\sigma(\omega) = \frac{4\pi^2}{\omega c}\sum_{\substack{\alpha>F\\ \beta\leq F}} |\mathfrak{D}_{\alpha\beta}(\omega)|^2\delta(\omega - \epsilon_\alpha + \epsilon_\beta). \tag{21}$$

To calculate the oscillator strengths, the discrete energy differences $E_n - E_0$ must also be calculated consistently in the RPAE. Denoting $\omega_s = \epsilon_\alpha - \epsilon_\beta$, $s \equiv (\alpha, \beta)$, we see that $\Pi^0_s(\omega_s)$ is singular and so Eq. (17) cannot be solved as it stands. We thus separate $\Pi^0(\omega)$ into two parts, one of them regular for some fixed transition $s_0 = (\alpha_0, \beta_0)$,

$$\Pi^{0\prime}_s(\omega) = (1 - \delta_{ss_0})\Pi^0_s(\omega), \tag{22}$$

and the other singular,

$$\Pi^{0\prime\prime}_s(\omega) = \delta_{ss_0}\Pi^0_s(\omega). \tag{23}$$

We then define[15]

$$\Gamma'(\omega) = U + U\Pi^{0\prime}(\omega)\Gamma'(\omega) \tag{24}$$

and

$$\mathfrak{D}'(\omega) = d + \Gamma'(\omega)\Pi^{0\prime}(\omega)d, \tag{25}$$

which are regular at $\omega = \omega_{s_0}$ by construction.

The effective interaction $\Gamma(\omega)$ and the renormalized vertex $\mathfrak{D}(\omega)$ are then

$$\Gamma(\omega) = \Gamma'(\omega) + \Gamma'(\omega)\Pi^{0\prime\prime}(\omega)\Gamma(\omega) \tag{26}$$

and

$$\mathfrak{D}(\omega) = \mathfrak{D}'(\omega) + \Gamma'(\omega)\Pi^{0\prime\prime}(\omega)\mathfrak{D}(\omega). \tag{27}$$

The matrix element corresponding to $s_0 = (\alpha_0, \beta_0)$ is

$$\mathfrak{D}_{s_0}(\omega) = \mathfrak{D}'_{s_0}(\omega)/[1 - \Pi^{0\prime\prime}_{s_0}(\omega)\Gamma'_{s_0s_0}(\omega)]. \tag{28}$$

Since $\omega > 0$ we have $n_{\beta_0} - n_{\alpha_0} = 1$; thus

$$\mathfrak{D}_{s_0}(\omega) = (\omega - \omega_{s_0})\mathfrak{D}'_{s_0}(\omega)/[\omega - \omega_{s_0} - \Gamma'_{s_0s_0}(\omega) - i\eta]. \tag{29}$$

$\mathfrak{D}'_{s_0}(\omega)$ is regular at $\omega = \omega_{s_0}$; $\mathfrak{D}_{s_0}(\omega)$ is not only regular there, but actually equal to zero. By comparing (26) and (27), we see that $\Gamma_{s_0s_0}(\omega)$ displays the same behavior. The pole of both matrix elements is displaced; it is given by the equation

$$\omega - \omega_{s_0} - \Gamma'_{s_0s_0}(\omega) = 0. \tag{30}$$

Since $\omega \approx \omega_{s_0}$, $\Gamma'_{s_0s_0}(\omega)$ is developed in a Taylor series around ω_{s_0} and only the first-order term is retained. An approximate solution of (30) is then obtained:

$$\omega = \omega_{s_0} + \Gamma'_{s_0s_0}(\omega_{s_0})\left(1 - \frac{\partial\Gamma'_{s_0s_0}}{\partial\omega}\bigg|_{\omega_{s_0}}\right)^{-1}. \tag{31}$$

In principle, one should solve (24) for $\Gamma'(\omega)$. Such an accuracy, nevertheless, is unnecessary, and the lowest-nonvanishing-order perturbation expansion in U is sufficient:

$$\Gamma'_{s_0 s_0}(\omega) \approx U_{s_0 s_0} + \sum_{s \neq s_0} |U_{s_0 s}|^2 \Pi^0_s(\omega) . \quad (32)$$

In calculating $\Gamma'_{s_0 s_0}$, $U_{s_0 s_0}$ is set equal to zero owing to the particular choice of single-particle states (see Sec. III). The residue of $S(\omega)$ at the displaced pole is determined as follows: We write

$$S(\omega) = \mathfrak{D}'(\omega)^\dagger \Pi^{0\prime\prime}(\omega) \mathfrak{D}(\omega) + d^\dagger \Pi^{0\prime}(\omega) \mathfrak{D}'(\omega) . \quad (33)$$

The second term in (33) is regular in the vicinity of $\omega = \omega_{s_0}$ and the correlation function may be written for $\omega \approx \omega_{s_0}$ as

$$S(\omega) = |\mathfrak{D}'_{s_0}(\omega)|^2 / [\omega - \omega_{s_0} - \Gamma'_{s_0 s_0}(\omega)] + (\text{regular part}) , \quad (34)$$

from which we see that

$$\mathrm{Res} S(\omega_p) = |\mathfrak{D}'_{s_0}(\omega_p)|^2 , \quad (35)$$

with $\omega_p \approx \omega_n$, is obtained as the solution of (30). The oscillator strength, Eq. (11), is then

$$f_n = (2/\omega_p) |\mathfrak{D}'_{s_0}(\omega_p)|^2 . \quad (36)$$

In the Feynman diagrams discussed so far a fermion line corresponds to the Green's function $G^0(\alpha; t - t')$ describing the free propagation, both forward ($t > t'$) and backward ($t < t'$) in time; therefore, the time ordering of interactions is irrelevant, and only topologically different diagrams are considered. Since a forward (backward) propagation corresponds to a particle (hole), it may be convenient to write $G^0 = G^0_> + G^0_<$, the first (second) term vanishing except for $\alpha > F$, $t > t'$ ($\alpha \leq F$, $t < t'$), and to associate $G^0_>$ ($G^0_<$) to a fermion line oriented in the sense of increasing (decreasing) time, such lines now being called particle (hole) lines. Then the time order of interactions remains irrelevant only to some extent, i.e., only those permutations are equivalent that do not change a particle line into a hole line, or vice versa. A certain number of these diagrams correspond to a single Feynman diagram, but their number is considerably smaller than that of the corresponding Goldstone diagrams, where different diagrams are obtained with any change in the time order of interactions. In the case of the RPAE this separation of G^0 leads to the separation of the polarization propagator, $\Pi^0 = \Pi^0_> + \Pi^0_<$. If a diagram contains only $\Pi^0_>$ this is a time-forward diagram; a diagram is time backward if at least one $\Pi^0_<$ appears in it.

The influence of the medium, consisting of a system of N particles in the ground state, on a particle moving through it is expressed by the irreducible self-energy part $\Sigma^*(\alpha, \omega)$.[14] If $G^0(\alpha, \omega)$ is expressed in the Hartree-Fock (HF) basis $\{\alpha\} \equiv \{\phi_i(\vec{r}), \phi_k^{N+1}(\vec{r})\}$, where the N functions $\phi_i(\vec{r})$ for $i \equiv \alpha \leq F$ are obtained as the ground-state solution of the self-consistent HF equations and $\phi_k^{N+1}(\vec{r})$ for $k \equiv \alpha > F$ is calculated in the frozen-core field of the HF ground state, then the first-order ω-independent term of Σ^* (i.e., the HF potential) is already included in G^0. Thus the HF self-consistent field essentially corresponds to an $(N+1)$-particle problem, except for $i \leq F$, where the terms corresponding to ith particle cancel due to the exchange. To describe an excited N-particle state an analysis of the two-particle Green's function in the particle-hole channel [or, equivalently, of $\Pi(\omega)$ in the case of the RPAE] becomes necessary. It turns out that is possible to transfer a part of the electron correlations from $\Gamma(\omega)$ to $\Pi^0(\omega)$ by replacing ϕ_k^{N+1} in $G^0_>$ with $\phi^N_{(i)k}$, calculated by omitting the term corresponding to the given hole i in the expression for the HF potential (the so-called potential V^{N-1}).[1,16] This choice effectuates the summation of all time-forward diagrams for $\Pi(\omega)$ diagonal in a given hole i. [While one should sum over all states corresponding to a fermion line in a diagram, we shall also call a "diagram" any term in this sum corresponding to some fixed state(s), such as the hole state i above]. Care must now be taken not to include once more the already summed diagrams (see Sec. III).

Ishihara and Poe[9] have considered in a general way the possibility of adding a conveniently chosen single-particle potential to the HF one such that the occupied states are not modified but that summation of an infinite class of diagrams having certain special structure is achieved, if the HF unoccupied states are replaced by the new ones. Our choice of $\phi^N_{(i)k}(\vec{r})$ single-particle states is a particular case of this method. For diagrams of the Goldstone type, where the time order of interactions is essential, they also proposed the multiple-basis-set technique, i.e., using two bases in the same diagram in order to sum an infinite class of diagrams which, between certain definite times, have structure permitting the summation by going to the new basis but are otherwise identical. For diagrams of the type used in this paper, where the time order is fixed only to some extent, the simultaneous use of two bases does not seem practicable.

There is an equivalent way of calculating $\sigma(\omega)$ and f_n in the RPAE. Starting directly from (3) in the dipole approximation, one can calculate the initial and final states and the excitation energies by solving the eigenvalue RPAE equation. This equation is obtained[14] by diagonalizing $\Pi(\omega)$; the eigenvalue equation determines the coefficients

$$C^{(n)}_{\lambda\mu} \equiv \langle \Psi_0 | c^\dagger_\mu c_\lambda | \Psi_n \rangle \quad (37)$$

and the excitation energies $\omega_n \equiv E_n - E_0$ (either $\lambda > F$, $\mu \leq F$, or $\lambda \leq F$, $\mu > F$). Writing

$$\langle\Psi_n|\sum_{i=1}^{N} d_i|\Psi_0\rangle = \sum_{\alpha\beta}\langle\alpha|d|\beta\rangle C^{(n)*}_{\alpha\beta} \tag{38}$$

and using (3), (13), (14), and the Lehmann representation of the polarization propagator, we see that this approach is exactly equivalent to the one we used. It was used by Altick and Glasgold in their calculations.[17] Alternatively, one might calculate the matrix elements $C^{(n)}_{\lambda\mu}$ by the perturbational development of the initial and final states. For the initial state, there is no difficulty as long as it is nondegenerate (closed or half-filled shells). For the excited state the situation is not so simple, because an excited state is usually degenerate. Here, in general, we must use the supplementary hypothesis, namely, that the adiabatic "turning off" gives approximately a given particle-hole state. Using the notation of Ref. 11, this means

$$\lim_{\eta\to 0} U_\eta(\infty, 0)|\Psi_n\rangle \approx c^\dagger_\lambda c_\mu|0\rangle . \tag{39}$$

If this is satisfied, we obtain[11]

$$\langle\Psi_n|\sum_{i=1}^{N} d_i|\Psi_0\rangle = \sum_{\alpha\beta}\frac{\Pi_{\lambda\mu,\alpha\beta}(\infty, 0)}{\Pi^0_{\lambda\mu,\alpha\beta}(\infty, 0)}\langle\alpha|d|\beta\rangle . \tag{40}$$

Further analysis of (40) gives the perturbation development used in Refs. 6–8. The nondegeneracy of $|\Psi_n\rangle$ brings about no difficulty if there is some symmetry (e.g., rotational invariance) which is not destroyed in the adiabatic turning off.[18] This is the case for the atoms we are studying here (excitations from an s shell); furthermore, we are using $\phi^{N(LS)}_{(i)k}(r)$ single-particle functions,[1,16] where the particle i and the hole k are coupled in an LS state of the atom.

III. CALCULATION

The single-particle wave functions by which the Coulomb interaction matrix elements are evaluated are calculated by using our Hartree-Fock programs,[19] self-consistently for the ground-state configuration (i.e., for the single-particle states below the Fermi energy), and, for excited discrete and continuous single-particle states in the HF frozen-core field of remaining electrons corresponding to the definite LS state of the atom, the functions $\phi^{N(LS)}_{(i)k}(\vec{r})$. Since these excited single-particle functions take into account the part of the RPAE correlations corresponding to all time-forward Goldstone-type diagrams diagonal in a given hole, the antisymmetrized Coulomb interaction matrix elements diagonal in the same hole have to be omitted (i.e., set equal to zero irrespective of their actual value[1]) in the relevant expressions, e.g., in the RPAE equation (17). Therefore in expression (32) for $\Gamma'_{s_0 s_0}(\omega)$ the first-order term in U ($U_{s_0 s_0}$) vanishes and the first nonvanishing term in the perturbation expansion is of second order.

To evaluate $\sigma(\omega)$, Eq. (21), and f_n, Eq. (36), the integral equation (17) for $\mathfrak{D}(\omega)$ has to be solved. Actually, for evaluation of f_n the equation for $\mathfrak{D}'(\omega)$ is to be solved, which is, according to (25) and (24), just the equation (17), but with $\Pi^{0\prime}(\omega)$ instead of $\Pi^0(\omega)$. After the usual multipole decomposition of the Coulomb interaction, the integration over angular variables as well as the summation over orbital magnetic quantum numbers and spins has been performed in the relevant equations.[1] It turns out then that the same equations are valid if the following replacements have been made: (a) single-particle–state quantum numbers $\alpha \equiv n_\alpha l_\alpha m_\alpha s_\alpha$ by $n_\alpha l_\alpha$; (b) relevant matrix elements by corresponding reduced matrix elements; and (c) the polarization propagator $\Pi^0_{\alpha\beta}(\omega)$ must be multiplied by $1/(2l+1)$, where l refers to lth multipole component of the Coulomb interaction [for the photoabsorption processes only the dipole ($l=1$) component contributes]. Also, the expressions (21) and (36), for $\sigma(\omega)$ and f_n, respectively, are to be multiplied by $\frac{1}{3}N_{n_\beta l_\beta}/(2l_\beta+1)$ ($\beta \le F$), where $N_{n_\beta l_\beta}$ is the number of electrons in the subshell.

The integral equation (17) is solved numerically. The integral over the energy variable has been replaced by a sum according to Simpson's rule, the sum being truncated at sufficiently high energy. The integration points are equidistant in $\kappa = \sqrt{2\epsilon}$, ϵ being the integration energy variable. The function under the integral has a pole [coming from $\Pi^0(\omega)$] and the corresponding integral has to be calculated in the sense of a principal value. To do this the numerical integration in the vicinity of the pole has been performed on the difference without a pole,[20]

$$f(\kappa) - r/(\kappa - \kappa_s), \tag{41}$$

r being the residue at the pole κ_s of the function $f(\kappa)$ under the integral. In such a way the integral equation (17) reduces to a system of algebraic equations and the problem of solving it is reduced to an inversion of a matrix.

IV. RESULTS AND DISCUSSION

The photoionization cross section and the oscillator strengths for the transitions from the ground states of helium, lithium, and beryllium atoms are calculated in the RPAE. The calculated r and ∇ forms of the cross section and the oscillator strengths coincide up to the error of calculations ($\lesssim 2\%$), as it should in the RPAE.

TABLE I. Calculated values f_{RPAE} of the oscillator strength in the RPAE. They are compared with the experimental values f_{exp} taken together with their respective error of measurements (given here in parentheses) of Wiese *et al.* (Ref. 21), except for the very recent experimental value for beryllium (Ref. 22). Certain results f_{MB} of other many-body calculations are given for comparison.

Atom	Transition	f_{RPAE}	f_{exp}	f_{MB}
He	$1s \rightarrow 2p$	0.252	0.276 (1%)	0.24 [a]
	$3p$	0.0703	0.0734 (1%)	0.071 [a]
	$4p$	0.0290	0.0302 (3%)	0.031 [a]
	$5p$	0.0147	0.0153 (< 10%)	•••
	$6p$	0.008 46	0.008 48 (< 10%)	•••
	$7p$	0.005 40	0.005 93 (< 10%)	•••
Li	$2s \rightarrow 2p$	0.758	0.753 (3%)	0.7575 [b]
	$3p$	0.004 07	0.005 52 (10%)	0.004 06 [b]
	$4p$	0.003 86	0.004 80 (10%)	0.003 84 [b]
	$1s \rightarrow 2p$	0.342	•••	•••
	$3p$	0.0562	•••	•••
	$4p$	0.0182	•••	•••
Be	$2s \rightarrow 2p$	1.36	1.34 ± 0.05	1.2540, [c] 1.378 [b]
	$3p$	0.0232	•••	0.016 76, [c] 0.002 27 [b]
	$4p$	0.001 10	•••	0.010 13, [c] 0.001 02 [b]
	$5p$	0.000 07	•••	0.005 49 [c]
	$6p$	$\lesssim 2 \times 10^{-6}$	•••	0.003 21 [c]
	$1s \rightarrow 2p$	0.374	•••	•••
	$3p$	0.0354	•••	•••
	$4p$	0.0117	•••	•••

[a] Many-body RPAE results from Ref. 23.

[b] Results of time-dependent HF approximation with the time-dependent external field, from Ref. 24.

[c] Many-body perturbation results from Ref. 5.

Our results for the oscillator strengths are presented in Table I together with the experimental values and other many-body calculations. There is good agreement with available experiments.

The results of our calculations of the photoionization cross section for the helium atom are shown in Fig. 3. Since the many-body perturbation theory results of Ishihara and Poe[7] differ from ours only slightly, they are not shown in Fig. 3. Our results always lie between their r- and ∇-form data. For the helium atom there is also the calculation of the cross section (and of oscillator strengths, as well) by Wendin[23] in the RPAE, differing from the present calculation essentially in the manner of solving approximately the RPAE equation (17), which has been solved iteratively in Ref. 23. Wendin's RPAE cross section practically coincides with ours. Wendin also corrected the RPAE by estimating the additional contribution from certain higher-order non-RPAE diagrams. As it is seen from Fig. 3, our calculation and Wendin's using the RPAE with some corrections agree with experiment[25,26] reasonably well.

The results of our calculations of the photoion-

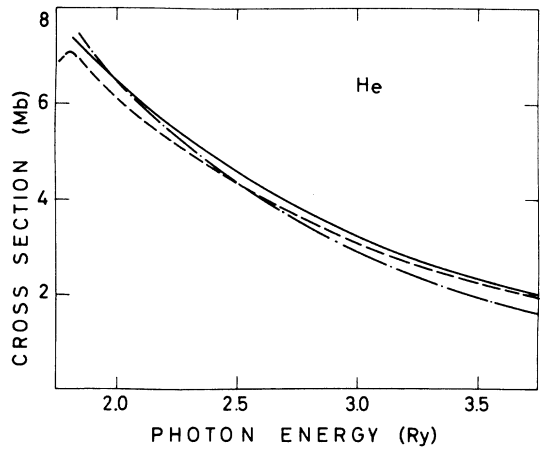

FIG. 3. Photoionization cross section for the helium atom ($1s \rightarrow \epsilon p$ transition). The solid curve represents the RPAE results of the present work, the dashed curve the RPAE with corrections of Wendin (Ref. 23), and the dot-dashed curve the averaged experimental results (Refs. 25 and 26). Since the many-body perturbation results of Ishihara and Poe (Ref. 7) (from threshold up to about 2.5 Ry) differ only slightly from the present ones, they are not shown here.

ization cross section for the lithium atom, for both $2s \rightarrow \epsilon p$ and $1s \rightarrow \epsilon p$ transitions, are presented in Fig. 4. The cross section for the transition from the outer subshell ($2s \rightarrow \epsilon p$) is presented in Fig. 5 and compared with the experimental data,[26-28] with the polarized-orbital-method calculation of Matese and LaBahn,[29] and with the very recent many-body perturbation calculation of Chang and Poe.[8] Our curve follows the trend of the experimental one, but the perturbation calculation of Chang and Poe agrees somewhat better with the experimental data. This probably can be ascribed to the EPV diagrams (their contribution being considerable in the lightest atoms). On the other hand, our results are closer to experiment than those of Matese and LaBahn, who simulate the many-body effects through the polarization potential.

The results of our RPAE calculation for the photoionization cross section for both the $2s \rightarrow \epsilon p$ and the $1s \rightarrow \epsilon p$ transitions of the beryllium atom are shown in Fig. 6. As for the lithium atom, the cross section for the transition from the outer subshell ($2s \rightarrow \epsilon p$ transition) only is shown in Fig. 7. It is compared with the earlier RPAE calculation of Altick and Glasgold[17] and with the many-body perturbation calculation of Kelly.[5] The difference between our results and those of Altick and Glasgold might be explained by the fact that they used Hartree instead of Hartree-Fock single-particle wave functions. Concerning the discrepancies between Kelly's many-body perturbational results[5] and ours, it is interesting to note that there is similar discrepancy between his and our HF results. This can probably be ascribed to Kelly's rather inconsistent choice of single-particle states. As

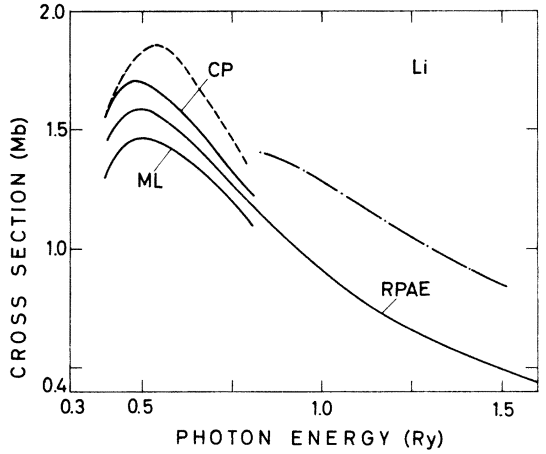

FIG. 5. Photoionization cross section for the transition from the outer subshell ($2s \rightarrow \epsilon p$) of the lithium atom. The curve denoted by RPAE represents our calculations; the CP curve represents the results of the many-body perturbation calculation of Chang and Poe (Ref. 8) (averaged ∇ and r curve, since the difference between them is rather small); the ML curve represents the results of polarized-orbital-method calculations of Matese and LaBahn (Ref. 29) (only the ∇ form; the r form practically coincides with our results); the dashed curve gives the experimental results of Ref. 27; and the dot-dashed curve gives those of Ref. 28.

there is no experiment to compare the calculations with, there is as yet no way to decide whose results are better.

There is a very recent calculation of oscillator strengths and cross sections for lithium and beryllium atoms by Stewart[23] in the time-dependent HF

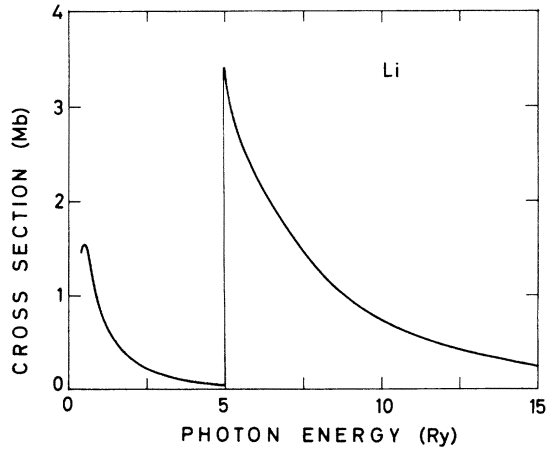

FIG. 4. Results of our RPAE calculation for the photoionization cross section of the lithium atom. The jump of the cross section at about 5.0 Ry corresponds to the (second) ionization threshold for the transition from the inner subshell ($1s \rightarrow \epsilon p$ transition).

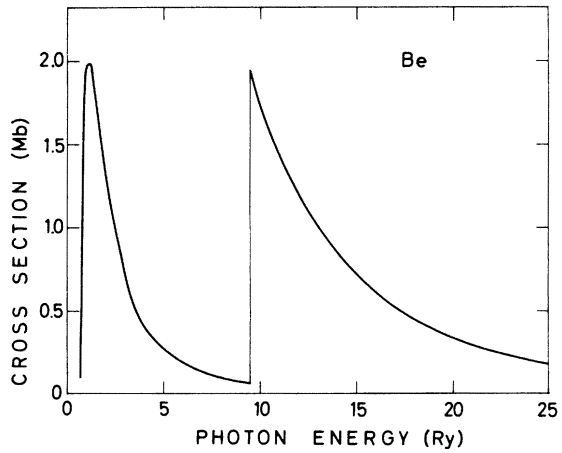

FIG. 6. Results of our RPAE calculations for the photoionization cross section of the beryllium atom. As for the lithium atom, the jump of the cross section at about 9.5 Ry corresponds to the (second) ionization threshold for the transition from the inner subshell ($1s \rightarrow \epsilon p$ transition).

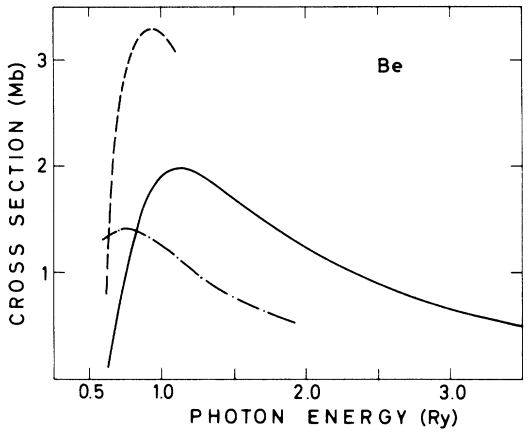

FIG. 7. Photoionization cross section for the transition from the outer subshell ($2s \rightarrow \epsilon p$) of the beryllium atom. The solid curve represents our RPAE calculations, the dashed curve represents the results of the RPAE calculations of Altick and Glasgold (Ref. 17), and the dot-dashed curve the results of perturbation calculations of Kelly (Ref. 5).

approximation with a time-dependent external field. While his oscillator strengths practically coincide with our results, as is seen in Table I, the cross sections (which are not shown here) disagree with our calculations and with available experiment; they lie below our results except in the region near the threshold.

The correlation effects in the outer-subshell transitions ($2s \rightarrow \nu p$, $\nu = n, \epsilon$) of the lithium atom on the oscillator strengths and the cross section belong completely to the intershell effects (only one electron in the $2s$ subshell), while in the inner-subshell transitions ($1s \rightarrow \nu p$) it was found that the nearly complete contribution comes from the intrashell RPAE correlations, the contribution from intershell effects being very small, amounting to only about 1%.

The effect of the intershell RPAE correlations in the outer-subshell transitions ($2s \rightarrow \nu p$, $\nu = n, \epsilon$) of the beryllium atom on the oscillator strengths and the cross section is not significant, but still amounts to about 10%. The intershell correlation effect in the inner-shell transitions ($1s \rightarrow \nu p$) is, as for the lithium atom, very small, amounting to about 1%. It should be mentioned that for all three atoms our calculated RPAE results satisfy the sum rule within a few percent.

ACKNOWLEDGMENTS

Two of the authors (Dj. Ž. and V. R.) would like to thank the Ioffe Institute for the hospitality extended to them. Thanks are due to I. Pavlin for many useful discussions.

[1] M. Ya. Amus'ya, N. A. Cherepkov, and L. V. Chernysheva, Zh. Eksp. Teor. Fiz. 60, 160 (1971) [Sov. Phys.—JETP 33, 90 (1971)].

[2] N. A. Cherepkov, L. V. Chernysheva, V. Radojević, and I. Pavlin, Can. J. Phys. 52, 349 (1974).

[3] M. Ya. Amus'ya, V. K. Ivanov, N. A. Cherepkov, and L. V. Chernysheva, Zh. Eksp. Teor. Fiz. 66, 1537 (1974) [Sov. Phys.—JETP 39, 752 (1974)].

[4] M. Ya. Amusia, N. A. Cherepkov, R. K. Janev, S. I. Sheftel, and Dj. Živanović, J. Phys. B 6, 1028 (1973).

[5] H. P. Kelly, Phys. Rev. 136, B896 (1964).

[6] E. S. Chang and M. R. C. McDowell, Phys. Rev. 176, 126 (1968).

[7] T. Ishihara and R. T. Poe, Phys. Rev. A 6, 116 (1972).

[8] T. N. Chang and R. T. Poe, Phys. Rev. A 11, 191 (1975).

[9] T. Ishihara and R. T. Poe, Phys. Rev. A 6, 111 (1972).

[10] M. Ya. Amusia, N. A. Cherepkov, Dj. Živanović, and V. Radojević, in *Proceeding of the Fourth International Conference on Vacuum Ultraviolet Radiation Physics, Hamburg, 1974* (Pergamon, New York, 1975).

[11] P. Nozières, *Theory of Interacting Fermi Systems* (Benjamin, New York, 1964).

[12] U. Fano and J. W. Cooper, Rev. Mod. Phys. 40, 441 (1968).

[13] H. P. Kelly and A. Ron, Phys. Rev. A 5, 168 (1972).

[14] A. L. Fetter and J. D. Walecka, *Quantum Theory of Many-Particle Systems* (McGraw-Hill, New York, 1971).

[15] A. B. Migdal, *Theory of Finite Fermi Systems and the Properties of the Atomic Nucleus* (Interscience, New York, 1967).

[16] M. Ya. Amusia, N. A. Cherepkov, R. K. Janev, and Dj. Živanović, J. Phys. B 7, 1435 (1974).

[17] P. L. Altick and A. E. Glasgold, Phys. Rev. 133, A632 (1964).

[18] H. P. Kelly, Phys. Rev. 144, 144 (1966).

[19] L. V. Chernysheva, N. A. Cherepkov, and V. Radojević, Comput. Phys. Commun. (to be published); see also A. F. Ioffe, Physical Technical Institute Report Nos. 486 and 487 (Leningrad, 1975) (unpublished).

[20] C. Bloch, in *Proceedings of the International School of Physics "Enrico Fermi," Course XXXVI,* edited by C. Bloch (Academic, New York, 1966), p. 394.

[21] W. L. Weise, M. W. Smith, and B. M. Glenon, *Atomic Transition Probabilities—Hydrogen through Neon,* Natl. Stand. Ref. Data Series, NBS 4 (U.S. GPO, Washington, D. C., 1966), Vol. I.

[22] I. Martinson, A. Gaupp, and L. J. Curtis, J. Phys. B 7, L463 (1974).

[23] G. Wendin, J. Phys. B 4, 1080 (1971).

[24] R. F. Stewart, J. Phys. B 8, 1 (1975).

[25] J. A. R. Samson, J. Opt. Soc. Am. 54, 842 (1964); R. B. Cairns and J. A. R. Samson, J. Geophys. Res. 70, 99 (1965).

[26]R. D. Hudson and L. J. Kiefer, At. Data 2, 205 (1971) (contains experimental data collected from Refs. 25, 27, and 28).
[27]R. D. Hudson and V. L. Carter, Phys. Rev. 137, A1648 (1965).
[28]R. D. Hudson and V. L. Carter, J. Opt. Soc. Am. 57, 651 (1967).
[29]J. J. Matese and R. W. LaBahn, Phys. Rev. 188, 17 (1969).